5º CONGRESSO BRASILEIRO DE PESQUISA E DESENVOLVIMENTO EM PETRÓLEO E GÁS

TÍTULO DO TRABALHO:

Gas-liquid displacement in channel with constrictions

AUTORES:

Oldrich Joel Romero

INSTITUIÇÃO:

Universidade Federal do Espírito Santo (UFES / CEUNES)

GAS-LIQUID DISPLACEMENT IN CHANNEL WITH CONSTRICTIONS

Abstract

Oil and gas are contained inside the porous rock or reservoir which is a porous medium. Fluid flow in porous media is a complex phenomenon. The path of the fluid flow is full of tortuosities, obstructions, abrupt changes in direction and it happens in a micro scale where the competition between capillary and viscous forces mainly governs the fluid flow. In order to increase the recovery factor or sustain the reservoir pressure, one common procedure is to pump gas or water through an injector well. The hydrocarbons (oil and gas) are displaced inside the porous media flowing to the bottom of the producer well and after through the tubing it arrives to surface facilities where is collected and processed, separating oil, gas, water and sediments. Because the main objective of any recovery process is minimize the amount of oil remaining in the rock, is important to know how the geometry, properties of the fluid, operational conditions, etc., influence in this process. In this work, the transient gas-liquid displacement of a Newtonian liquid inside channels with sinusoidal obstructions is analyzed numerically. The influence of the degree and number of the constriction in the liquid film thickness variation is determined at different process conditions by solving the transient, two-dimensional, viscous free surface liquid flow in the channel. The shape of the interface needs to be determined as part of the solution. The set of differential equations and boundary conditions posed in the unknown domain had to be transformed to an equivalent set defined in a known reference domain. The system of equations, with appropriate boundary conditions, was solved by the Galerkin/finite element method, and an implicit time integration. The preliminary results show the bubble evolution and the influence in the pressure and tip velocity.

Keywords: constrictions, free-surface, oil recovery, Galerkin/FEM.

1. Introduction

Fluids entering the wellbore from the reservoir can range from an undersaturated oil to single-phase gas. Free water can accompany the fluids as a results of water coning, water flooding, or production of intersticial water. Alternative, a free gas saturation in an oil reservoir can result in a gas/liquid mixture entering to the well. Retrograde condensation can result in hydrocarbon liquids condensing in a gas condensate reservoir.

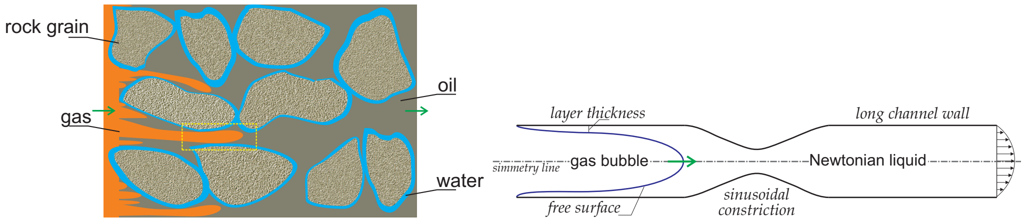

Figure 1: Schematic microscopic representation of the porous media containing oil, gas and connate water. Left side: Sketch of the physical model

The two-phase immiscible flow through oil saturated consolidated porous media is of great practical interest, specially in enhanced oil recovery (Slattery, 1974). There are other practical applications and physical operations where the common basic characteristic is the gas displacing a viscous liquid, such as the monolith reactors, the pulmonary airway reopening, the gas-assisted injection molding. Many authors with quite different approaches have been studied this multifaceted problem.

Immiscible flooding with gas is considered to be one of the most effective enhanced oil recovery processes applicable to light and medium oil reservoirs. Fig. 1 shows a oil being displaced by gas, where the basic interest is the shape of the interface during displacement.

In spite of the importance of the subject, prior studies were mainly related to the gas-liquid displacement in straight tubes and channels, and the gas bubble formed while displacing the liquid was considered semi-infinite, making the motion steady, see for example Taylor (1961), Bretherton (1961), Cox (1962). A few numerical studies have been conducted related with the flow in constricted geometries.

The Taylor bubble problem consist of two fluids: a gas of negligible density in a interior of the bubble and an incompressible Newtonian fluid in the exterior of the bubble. The bubble is symmetric and infinitely long which. Comprehensible reviews on capillary displacements are available in the literature, see for example Olbricht (1996) and Stark and Manga (2000).

Fairbrother and Stubbs (1935) calculated film thickness h from direct measurements of backflow in capillary tubes and established remarkably simple empirical correlation for moving bubbles sufficiently long, i.e. $> 3r$, so that the bubble can be considered cylindrical: $h = (r/2)\sqrt{Ca}$. The dimensional group $Ca = U_b\mu/\sigma$ is the capillary number and represents the relation between the forces increasing distortion of the bubble and hence an increase of h (will increase with bubble velocity U_b and fluid viscosity μ), and the forces resisting distortion (will increase with bubble curvature $1/r$ and surface tension σ), Marquessault and Mason (1960).

The rock pores has been extensively studied approximating the tortuous path as a single straight tube by several researchers Olbricht (1996), Stark and Manga (2000) or in a Helle-Shaw cell. Also, this complex porous media have approximated with a tube of varying cross section for single phase flow. However, studies with two-phase flows in tubes or channels with constrictions are rare. It kind of geometry is appropriated for describe the converging-diverging character of each path of the reservoir.

The objective of the work presented in this paper is to presents a transient numerical simulation of the dynamic of a gas liquid displacement in channels whit constrictions based on the numerical technique presented in Romero and Carvalho (2008). The main focus of this initial research is a study of the influence of the intensity of the channel constriction upon the gas-liquid interface and the obtain a complete picture of the dynamic evolution of the bubble surface and flow field ahead and behind its tip. Because the fluid flow is very slow, around 1 ft/day, is possible to assume that in this approach the inertial terms are negligible when compares with the viscous terms, which means that the Reynolds number (inertial over viscous forces) is zero in our research.

2. Problem formulation

2.1 Governing equations, boundary and initial conditions

Figure 2 shows the domain with a gradually contraction between the upper wall and its symmetry line. At the begin, the domain is completely filled by the Newtonian liquid forming a flat free surface at the entrance of the channel. The liquid is displaced by a pressurized gas from left to right which is increased abruptly from zero to a prescribed value causing a continuous deformation of the free surface, a bubble gas is created which invades the varying slot channel diminishing the volume of liquid. A three-phase contact line is formed in the upper left side corner, we considered this contact line pined to the corner, for a deep discussion about this subject refers to Romero et al. (2006). A film thickness is deposited in the wall.

The governing equations are written in a two-dimensional rectangular coordinates where x and y are the horizontal and vertical co-ordinates, respectively. Because the problem is considered symmetrical, as shown in Fig. 2, only half of the domain is considered, reducing the computational effort dispensed to solve the problem.

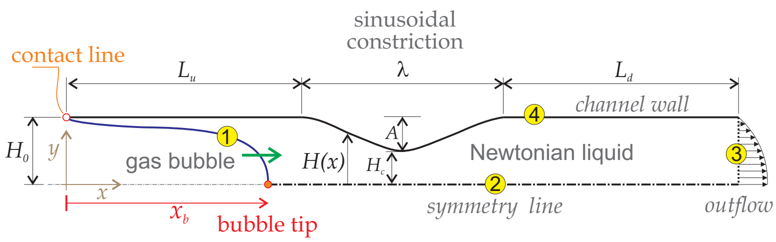

Figure 2: Flow domain and boundary conditions for gas-liquid displacement in a constricted channel.

The gap of the channel varies in the axial direction, x, according to

$$
\begin{aligned}
 &= H_0, \qquad 0 \le x < L_u \\
H(x) &= H_0 - A\, sin(2\pi x/\lambda), \qquad L_u \le x \le L_u + \lambda \\
 &= H_0, \qquad L_u + \lambda < x \le L_u + \lambda + L_d,
\end{aligned}
\tag{1}
$$

where A and λ represent the amplitude and wavelength of corrugation, respectively. The planar geometry consists of three parts: an introductory segment of constant gap H_0 and length L_u, a harmonically varying middle part of length λ, and a exit segment of constant gap H_0 and length L_d. The minimum gap is H_c.

The equations governing the transient, two-dimensional, incompressible flow field in the absence of inertial effects (i.e., when Reynolds number $\ll 1$) can be written as

$$\nabla \cdot \mathbf{v} = 0, \tag{2}$$

$$\rho \left(\frac{\partial \mathbf{v}}{\partial t} + \mathbf{v} \cdot \nabla \mathbf{v} \right) - \nabla \cdot \mathbf{T} = 0, \tag{3}$$

where $\mathbf{v} = (u, v)$ and pressure p are the velocity and pressure fields, respectively; ρ is the liquid density. The total stress tensor for Newtonian liquids is $\mathbf{T} = -p\mathbf{I} + \mu[\nabla \mathbf{v} + (\nabla \mathbf{v})^{\mathrm{T}}]$, where μ is the liquid dynamic viscosity and the superscript $^{\mathrm{T}}$ means transpose. Because of the small dimensions of the flow, body forces are usually neglected.

The flow domain and its boundaries are labelled in Fig. 2, the corresponding boundary conditions are:

(1) At the inflow plane, where the gas displaces the liquid, there is a free surface; the velocity field should satisfy a local force balance between the traction in the liquid, the capillary pressure and the gaseous pressure, given by Eq. (4). It is assumed that the gas viscosity is much smaller than the liquid viscosity, leading to vanishing shear stress along the gas-liquid interface

$$\mathbf{n}_{fs} \cdot \mathbf{T} = \sigma \frac{d\mathbf{t}_{fs}}{ds} - \mathbf{n}_{fs}\, P_{in}, \tag{4}$$

where σ is the liquid surface tension, $\mathbf{t}_{fs}$ and $\mathbf{n}_{fs}$ are the local unit tangent and unit normal vectors to the free surface (identified by the subscript $_{fs}$), $d\mathbf{t}_{fs}/ds$ represents the curvature of the meniscus and s the arc-length coordinate along the free surface. P_{in} is the pressure imposed at the free surface located in the entrance of the channel. A step change in this value is applied: at $t = 0$ pressure is suddenly increased to $P_{in} = 3.63$ and remains constant until the end of the computations, this is when the last time t_{LAST} is reached. Also, there is no mass flow rate across the gas-liquid interface, and following Christodoulou and Scriven (1992) we use the kinematic condition considering the mesh velocity $\overset{\circ}{\mathbf{x}}$

$$\mathbf{n}_{fs} \cdot \left(\mathbf{v} - \overset{\circ}{\mathbf{x}} \right) = 0, \tag{5}$$

(2) Along the symmetry line, both the shear stress and the vertical velocity vanish

$$\mathbf{n} \cdot \mathbf{v} = 0, \quad \mathbf{n} \cdot (\mathbf{T} \cdot \mathbf{t}) = 0, \tag{6}$$

$\mathbf{n}$ and $\mathbf{t}$ are the unit vector normal and tangent to the boundary.

(3) At the outflow plane, fully developed parallel rectilinear flow and pressure imposed $P_{out} = 0$ are used

$$\mathbf{n} \cdot (\nabla \mathbf{v}) = 0, \quad p = P_{out}, \tag{7}$$

the outflow plane was located at a distance equal to $5H_0$ downstream from the constriction. Changes on its location did not affect the steady state solution.

(4) The no-slip and no-penetration conditions applies along the channel walls

$$u = 0, \quad v = 0. \tag{8}$$

Finally, an initial condition is needed in order to solve the transient flow problem. In this work, we assume the initially there is no flow and the pressure field is uniform in all the domain

$$\mathbf{v}(t = 0) = \mathbf{0}, \quad p(t = 0) = 0. \tag{9}$$

2.2 Geometries

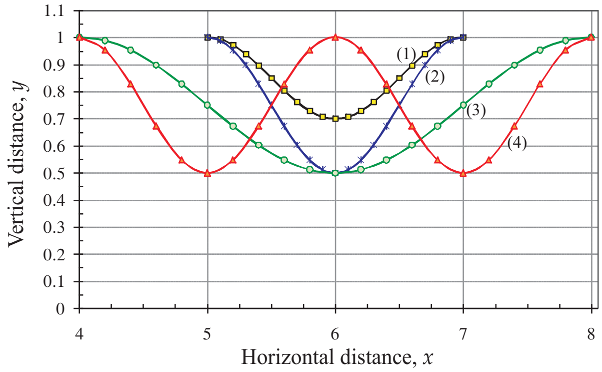

Figure 3: Configurations of the channel constriction.

The transient, two-dimensional flow in the Helle-Shaw cell was analyzed at different amplitudes and frequencies of the imposed oscillation. In order to explore the effect of the geometry of the constriction, four different wall configurations were considered; they are shown in Fig. 3.

3. Solution method

The primary difficulty in applying the finite element method (FEM) to free-surface problems is the need to specify a procedure for constructing a mesh over the domain, the shape of which is *a priori* unknown. For those FEM problems which involve free surfaces that move during the computation, an initial mesh can be updated simply by using a continuous deformation algorithm which maintains the same mesh connectivity throughout the problem. In preserving connectivity, we also preserve the sparsity patterns of the various matrices that arise in the discretisation solution of the problem, e.g. stiffness and mass matrices, Jacobians, etc., with obvious efficiency advantages. The shape of the interface needs to be determined as part of the solution. Several schemes for obtaining the shape of the free surface together with the velocity and pressure fields are available. The system of governing equations, together with the appropriate boundary conditions was solved by Galerkin's method with quadrilateral finite elements. The temporal discretization of the set of ordinary differential-algebraic equations, followed a predictor-corrector algorithm. The predictor step consists of a forward Euler method and the corrector step consists of a first-order fully implicit Euler method, which is unconditionally stable. The system of ordinary differential-algebraic equations is reduced to simultaneous algebraic nonlinear equations for the coefficients of the basis functions of all the fields. At each time step, the resulting set of nonlinear algebraic equations was solved simultaneously by Newton's method with an initial estimate resulting from an explicit Euler step from the solution at the previous two time steps

Additional details of this derivation we refer to Romero and Carvalho (2008) where is presented a numerical study of coating flows under periodic disturbances, additionally de Santos (1991) and Christodoulou and Scriven (1992).

4. Results and discussion

The Newtonian liquid initially occupies the entire domain. At the beginning of the computations $t = 0$ the gas-liquid interface is considered flat. A step change in the pressure P_{in} is applied on the gas side of the gas-liquid interface at the entrance of the channel throughout the

Eq. (4) forcing the transient penetration of the gas bubble into the varying slot crated by the neck in the parallel plates. Because of that, the steady state is not reached and the flow domain changes in shape and size, demanding a reconstruction of the mesh several times. Differently from another approaches –Fairbrother and Stubbs (1935), Fairbrother and Stubbs (1935), Fairbrother and Stubbs (1935)– where the wall is and the bubble is static, in our work the wall is fixed. Because the prescribed pressure at the exit of the domain is $P_{out} = 0$, the applied pressure difference remains constant. But, once the bubble moves along the slot in direction to the output boundary, the volume of the liquid in the domain decrease reducing the resistance to the flow. This results in an acceleration of the flow field.

Computations are performed until $t = t_{LAST}$ has been reached. The last time, t_{LAST}, is different for each geometry because the mesh deformation limits is influenced by the type of constriction present in the channel.

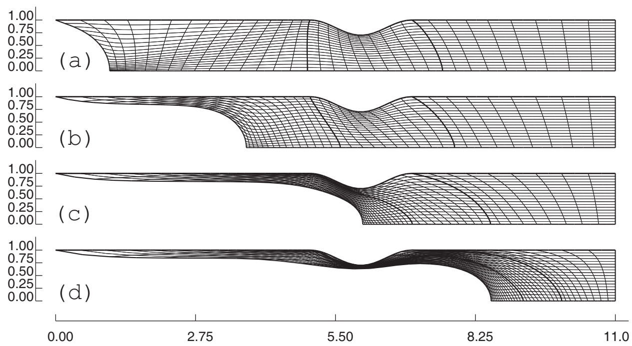

Figure 4: Mesh bubble evolution at different time instants as a function of the time step Δt: (a) $12\Delta t$, (b) $48\Delta t$, (c) $71\Delta t$ and (d) $86\Delta t$. The geometry for this case is the number (1) showed in Fig. 3

A gas bubble moving at constant pressure through a constricted noncircular capillary is illustrated in Fig. 4. As the bubble invades the constriction, the mean curvature of the gas-liquid interface increases, so that the bubble front may squeeze into the constriction. After the front has passed the tightest part, or neck, of the constriction, the interfacial curvature begins to decrease. As commented by Ransohoff et al. (1987) "this drop in curvature, if sufficiently large, initiates a wetting-liquid pressure gradient directed from the front of the bubble to the neck of the constriction. Liquid flows into the constriction, and eventually enough liquid may accumulate at the constriction neck to block the pore and snap-off a gas bubble". Snap-off occurs when wetting fluid (liquid) accumulates by capillary action in a pore throat occupied by non-wetting phase (gas) and then bridges across the throat to block flow. Capillary pressure must be high enough for gas to invade the throat, but then fall by about a factor of two for liquid to re-invade the throat, which means that if the pore body radius is at least about twice the throat radius, snap-off occurs in agree with the basic Roof's criteria, (Rossen, 2000).

A comparison of bubble position at the last time of computation for the different channel undulation are shown in Fig. 5. In the four cases, the mesh is strongly deformed around the constricted section and when it passes through the constriction. Convergence of the solution process is lost at time instants which are functions of the intensity of the channel variation. The remaining film has a nonuniform thickness distribution being thicker before contractions.

Fig. 6 shows the time evolution of the bubble tip position for the four channel configurations. The bubble tip moves toward the channel exit monotonically. The evolution of the tip exhibits small-amplitude oscillations. The time required for the bubble tip to reach a certain position in the tube increases with the intensity of the undulation variation.

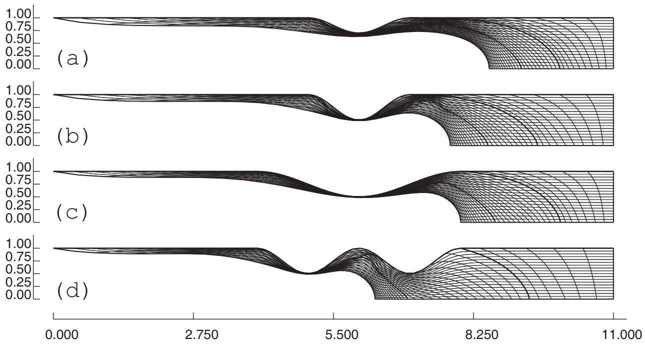

Figure 5: Comparison of the mesh deformation at the last time of computing: (a) $86\Delta t$, (b) $115\Delta t$, (c) $146\Delta t$ and (d) $150\Delta t$; for geometries (1), (2), (3) and (4) respectively.

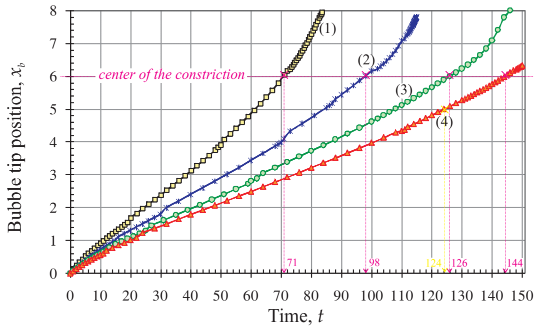

Figure 6: Evolution of the bubble tip position.

A strong decline of the pressure of the bubble tip is observed at the beginning of the process, as shown in Fig. 7, after that it declines linearly until it arrives close to the constricted section where pressure decrease is stronger, since more energy is consumed there. In addition, there is a time delay in the response of the pressure at the bubble tip, it has a minimum after the bubble front has passed through the channel minimum. For example, the bubble reaches the constriction at $t = 71\Delta t$, and the pressure is minimized at $t = 75\Delta t$. The response of the bubble tip velocity is also presented. The bubble tip velocity is almost constant before the constriction, after the bubble past the constriction, it immediately expands accelerating.

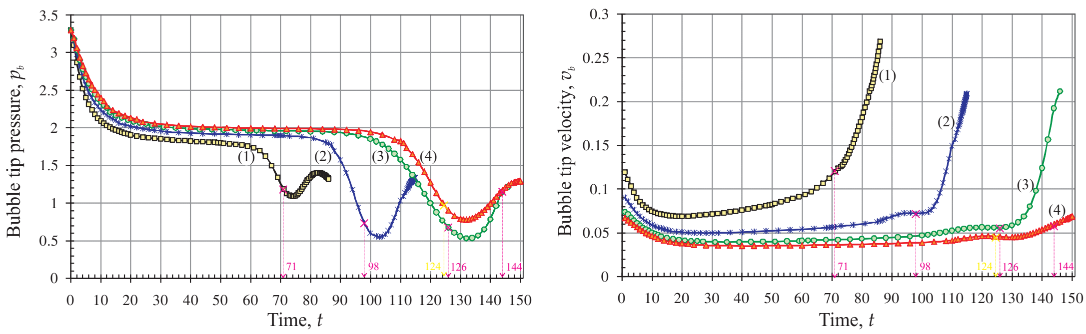

Figure 7: Pressure and velocity of the bubble tip.

5. FINAL REMARKS

Our intention in this work has been to present the numerical technique and the first results obtained when applied to the transient gas-liquid displacement. Certainly is necessary to improve the treatment of this results, especially its presentation using dimensionless parameters. This will be done in the future, when a more refined mesh and a smaller time step will be selected, and running each case in a more powerful computer.

REFERENCES

Bretherton, F. P., 1961. The motion of long bubbles in tubes. *J. Fluid Mech.*, vol. 10, pp. 166–188.

Christodoulou, K. N. & Scriven, L. E., 1992. Discretization of free surface flows and other moving boundary problems. *Journal of Computational Physics*, vol. 99, pp. 39–55.

Cox, B. G., 1962. On driving a viscous fluid out of a tube. *J. Fluid Mech.*, vol. 14, pp. 81–96.

de Santos, J. M., 1991. *Two-phase cocurrent downflow through constricted passages*. PhD thesis, University of Minnesota, MN, USA.

Fairbrother, F. & Stubbs, A., 1935. Studies in electroendosmosis. part vi. the bubble-tube methods of measurement. *J. Chem. Soc.*, vol. 1, pp. 527529.

Marquessault, R. N. & Mason, S. G., 1960. Flow of entrapped bubbles through a capillary. *Ind. and Engineering Chem.*, vol. 52, n. 1, pp. 79–84.

Olbricht, W. L., 1996. Pore-scale prototypes of multiphase flw in porous media. *Annu. Rev. Fluid Mech.*, vol. 28, pp. 187–213.

Ransohoff, T. C., Gauglitz, P. C., & Radke, C. J., 1987. Snap-off of gas bubbles in smoothly constricted noncircular capillaries. *AIChE J.*, vol. 33, n. 5, pp. 753–765.

Romero, O. J. & Carvalho, M. S., 2008. Response of slot coating flows to periodic disturbances. *Chemical Engineering Science*, vol. 63, n. 8, pp. 2161–2173.

Romero, O. J., Scriven, L. E., & Carvalho, M. S., 2006. Effect of curvature of coating die edges on the pinning of contact line. *AIChE J.*, vol. 52, pp. 447–455.

Rossen, W. R., 2000. Snap-off in constricted tubes and porous media. *Colloids and Surfaces A*, vol. 166, pp. 101–107.

Slattery, J. C., 1974. Interfacial effects in the entrapment and the displacement of residual oil. *AIChE J.*, vol. 20, pp. 1145–1154.

Stark, J. & Manga, M., 2000. The motion of long bubbles in a network of tubes. *Transport Porous Media*, vol. 40, pp. 201–218.

Taylor, G., 1961. Deposition of a viscous fluid on the wall of a tube. *J. Fluid Mech.*, vol. 10, pp. 161–165.